JIPB Journal of Integrative Plant Biology

Overexpression of *INCREASED CAMBIAL ACTIVITY*, a putative methyltransferase, increases cambial activity and plant growth

Hyunsook Kim[1], Mikiko Kojima[3], Daeseok Choi[1], Soyoung Park[1], Minami Matsui[2], Hitoshi Sakakibara[3] and Ildoo Hwang[1]*

[1]Department of Life Sciences, Pohang University of Science and Technology, Pohang 790-784, Korea, [2]Synthetic Genomics Research Team, Biomass Research Cooperation Division (BMEP), RIKEN Center for Sustainable Resource Science (CSRS), Tsurumi, Yokohama 230-0045, Japan, [3]Riken Center for Sustainable Resource Science (CSRS), Tsurumi, Yokohama 230-0045, Japan. *Correspondence: ihwang@postech.ac.kr

ABSTRACT Cambial activity is a prerequisite for secondary growth in plants; however, regulatory factors controlling the activity of the secondary meristem in radial growth remain elusive. Here, we identified *INCREASED CAMBIAL ACTIVITY* (*ICA*), a gene encoding a putative pectin methyltransferase, which could function as a modulator for the meristematic activity of fascicular and interfascicular cambium in *Arabidopsis*. An overexpressing transgenic line, *35S::ICA*, showed accelerated stem elongation and radial thickening, resulting in increased accumulation of biomass, and increased levels of cytokinins (CKs) and gibberellins (GAs). Expression of genes encoding pectin methylesterases involved in pectin modification together with pectin methyltransferases was highly induced in *35S::ICA*, which might contribute to an increase of methanol emission as a byproduct in *35S::ICA*. Methanol treatment induced the expression of GA- or CK-responsive genes and stimulated plant growth. Overall, we propose that ectopic expression of *ICA* increases cambial activity by regulating CK and GA homeostasis, and methanol emission, eventually leading to stem elongation and radial growth in the inflorescence stem.

Keywords: Cambial activity; cytokinin; gibberellin; methanol; methyltransferase; pectin; shoot growth
Citation: Kim H, Kojima M, Choi D, Park S, Matsui M, Sakakibara H, Hwang I (2016) Overexpression of *INCREASED CAMBIAL ACTIVITY*, a putative methyltransferase, increases cambial activity and plant growth. **J Integr Plant Biol** 58: 874–889 doi: 10.1111/jipb.12486
Edited by: Ivan Galis, Okayama University, Japan
Received Apr. 22, 2016; **Accepted** Jun. 20, 2016
Available online on Jun. 20, 2016 at www.wileyonlinelibrary.com/journal/jipb

High-Impact Article

Free Access

INTRODUCTION

Vascular tissues of higher plants are important not only for transporting water, minerals, photoassimilates, and signaling molecules but also for physically supporting the plant body (Scarpella and Meijer 2004). In the inflorescence stem, the vasculature includes vascular bundles, consisting of procambium, phloem, and xylem, during primary growth. *Fascicular cambium*, originating from procambium, is bidirectionally differentiated into xylem and phloem. After the development of primary xylem and phloem tissues, interfascicular cambium is established following asymmetric periclinal cell divisions and eventually fused with fascicular cambium to form a circular cambial structure called vascular cambium that provides a means of radial thickening for secondary growth. This growth is of an economically important biological process as it results in the production of biomass, is a renewable and sustainable source of energy. Thus, the regulation of cambial activity could be one of the best strategies for maximizing cellulose biomass yield.

The development of vascular tissues is tightly regulated during the plant life cycle (Baucher et al. 2007; Caño-Delgado et al. 2010), and phytohormones are important regulatory factors of vascular cambial activity (Elo et al. 2009; Nieminen et al. 2012; Miyashima et al. 2013). Auxin predominantly distributed in the cambial zone regulates both cambial activity and secondary growth (Uggla et al. 1996; Uggla et al. 1998; Ko et al. 2004; Nilsson et al. 2008; Ilegems et al. 2010; Etchells et al. 2015). Polar auxin transport regulates several regulators in vascular development. PHLOEM INTERCALATED WITH XYLEM (PXY)/TRACHEARY ELEMENT DIFFERENTIATION INHIBITORY FACTOR (TDIF) RECEPTOR (TDR) and TDIF function as a receptor–ligand pair to induce *WUSCHEL-RELATED HOMEOBOX4* (*WOX4*) and *WOX14* for promoting cambial activity in an auxin-dependent manner (Fisher and Turner 2007; Hirakawa et al. 2008; Hirakawa et al. 2010; Suer et al. 2011; Etchells et al. 2013). Cytokinin (CK) is another important regulator of cambial cell proliferation. CK level is highly correlated with cambial activities of both root and shoot (Matsumoto-Kitano et al. 2008; Nieminen et al. 2008), and perturbation of CK signaling impaired the maintenance of cambial cells (Mähönen et al. 2000; Yokoyama et al. 2007; Hejátko et al. 2009). Consistently, genes involved in CK biosynthesis, translocation, and signal transduction are abundantly expressed in the cambial zone (Miyawaki et al. 2004; Hirose et al. 2005; Zhao et al. 2005; Nieminen et al. 2008; Ko et al. 2014; Zhang et al. 2014). Gibberellin (GA) modulates cambial activity to differentiate into xylem tissues, thus influencing the number or length of xylem fibers (Eriksson et al. 2000; Funada et al. 2008; Dayan et al. 2012), an observation consistent with high level of bioactive GAs in xylem initial cells (Israelsson et al. 2005). GA also functions as a

leaf-derived mobile signal in xylem expansion (Ragni et al. 2011). Interestingly, GA biosynthesis in poplar was transiently induced at the early stage of cambial reactivation during spring, suggesting that GA is involved in season- or age-dependent regulation of cambial growth in tree species (Druart et al. 2007).

Cell wall mostly contributes to plant biomass production and its modification is also related to plant growth. Homogalacturonan (HG), the most abundant pectic polysaccharide, is a critical element of the primary cell wall in plants. For example, HG modification by disrupting genes encoding putative pectin methyltransferases, such as *tumorous shoot development2* (*tsd2*)/*quasimodo2* (*qua2*) and *cotton golgi-related 2, 3* (*cgr2 cgr3*) mutants, conferred growth retardation and overexpression of *CGR2* or *CGR3* increased size and fresh weight of rosette leaves (Krupková et al. 2007; Held et al. 2011; Kim et al. 2015).

In this study, we showed that ICA, a putative pectin methyltransferase, could alter the levels of several hormones including CKs and GAs in *Arabidopsis*, leading to increased cambial activity and plant growth.

RESULTS

Isolation of *35S::ICA* with increased cambial activity and biomass production of the shoot

To identify regulators of cambial activity, we screened an *Arabidopsis* FOX line collection generated by a novel gain-of-function system using full-length cDNAs, as previously described (Ichikawa et al. 2006). The bases of inflorescence stems from 4,500 transgenic plants were sectioned at the stage of first silique development, and transgenic lines with altered vascular development were selected using the light microscope. One of the lines showed prominently increased layers of cambial cells and was named "*35S::ICA*".

In Col-0 plants, the vascular system was organized in ordered and discrete bundles separated by the interfascicular region in the inflorescence stem (Figure 1A). Fascicular cambium was located between the phloem and xylem in each bundle, but the interfascicular cambium between vascular bundles was not distinctly developed at the stage of first silique development (Figure 1A). In *35S::ICA*, the ordered vascular patterning was not changed, but it had a thick, fasciated inflorescence stem, and the interfascicular cambium was already visible between vascular bundles (Figure 1A). Secondary xylems and phloems were also observed in *35S::ICA* interfascicular regions (Figure 1A). In comparison with Col-0, the number of xylem and phloem cells was markedly increased (by >20%) and that of cambial cells was significantly increased (by 3.4-fold) in *35S::ICA* (Figure 1B). Cell size was not changed in the phloem and cambium but slightly increased in the xylem of *35S::ICA* (Figure 1C). The number of vascular bundles was 7.4 ± 0.3 (mean $\pm$ *SE*) in Col-0 but 9.2 ± 0.3 in *35S::ICA* (Figure 1D). The stem diameter of *35S::ICA* was particularly increased by 30% at the stage of the first silique development, and remained larger than that of Col-0 throughout the life cycle (Figure 1E, F).

We then further analyzed the growth phenotypes of *35S::ICA* with respect to biomass production. The total length of the vegetative stem internode was significantly longer in *35S::ICA* than in Col-0 plants (Figure 2A), and the number of vegetative internodes in the main inflorescence stem was significantly increased in *35S::ICA* (Figure 2B), indicating that the capacity for lateral shoot branching along the primary shoot axis is highly increased in *35S::ICA*. In addition, a significant increase in stem height at the first and sixth silique stages (Figure 2C) clearly correlated with the increased number and overall length of vegetative internodes, and the final height of *35S::ICA* was significantly greater than that of Col-0 by 8% (Figure S1A). The fresh and dry weight of the inflorescence stem in *35S::ICA* were significantly increased compared with those in Col-0 at the first and sixth silique stages (Figure S1B, C), owing mainly to the increased fresh and dry weight of vegetative internodes and axillary stems in *35S::ICA* as measured at the sixth silique stage (Figures 2D, S1D). Moreover, fresh weight of rosette leaves more expanded in *35S::ICA* than Col-0 was significantly increased in *35S::ICA* (Figures 2E, F, S1E, F). Consistently, both the fresh and dry weight of *35S::ICA* shoot were also significantly increased compared with those of Col-0 shoot at the first and sixth silique stages (Figures 2G, S1G, H). We then examined the root growth in 6-day-old *35S::ICA* seedlings; not only the length and cell number of meristemic zone but also the length and diameter of primary roots in *35S::ICA* were similar to those in Col-0 (Figure S2).

Endogenous CK levels are highly increased in *35S::ICA* during the shoot development

To understand how *35S::ICA* affects the cambial activity, we first analyzed levels of endogenous plant hormones in various tissues at different vegetative stages and six siliques stage and found that active CKs were particularly increased in all developmental stages measured in *35S::ICA* (Table S1). In vegetative stages, only CKs, especially CK nucleobases and CK ribosides, were markedly increased in *35S::ICA* compared with Col-0 (Figure 3A, B). CK nucleobases were increased in internodes, axillary buds, and cauline leaves at the sixth silique stage of *35S::ICA* (Figure 3C). In addition, CK ribosides were accumulated abundantly in all measured tissues (Figure 3D). Interestingly, both tZ- and cZ-type CKs were increased in *35S::ICA* inflorescence stems, but iP-type CKs were slightly decreased in inflorescence internodes, axillary stems, and leaves, although the total amount of CKs was higher in *35S::ICA* than in Col-0 (Figure S3). In agreement with the elevated CK levels in *35S::ICA*, the CK-responsive genes *ARR5*, *ARR6*, and *ARR7* were upregulated in *35S::ICA* (Figure 3E). The microarray analysis also revealed that many CK-inducible genes (Bhargava et al. 2013) were upregulated in *35S::ICA* (Figure S4). Overall, these results suggest that the modulation of CK levels could be a major physiological factor in growth phenotype change in *35S::ICA*.

We also profiled endogenous GAs, precursor (GA_{53}, GA_{44}, GA_{19}, GA_{20}, GA_{24}, and GA_9), bioactive (GA_1, GA_3, and GA_4), and deactivated (GA_8) GAs, in Col-0 and *35S::ICA* (Table S2). The GA level was not altered in *35S::ICA* in vegetative stages; however, at the sixth silique stage, most precursor GAs were markedly increased in *35S::ICA* plants compared with Col-0 plants (Table S2). The total amount of GAs were markedly increased in all tissues of *35S::ICA*, except for axillary stems (Figure 4A). The level of GA_4, the critical bioactive form in the early reproductive stage in *Arabidopsis* (Sponsel et al. 1997;

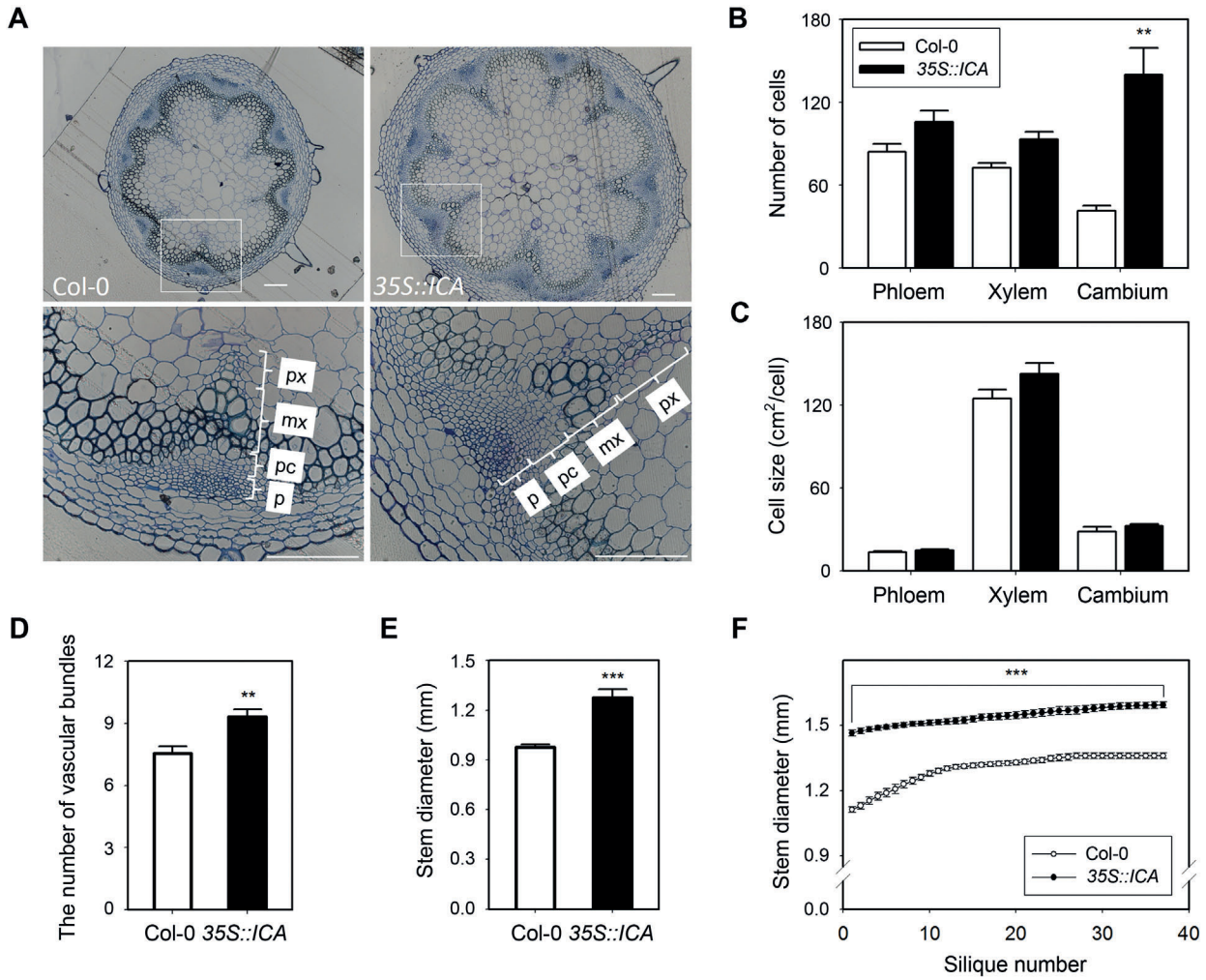

Figure 1. *35S::ICA* increases cambial activity biomass production

(A) *35S::ICA* (right) shows the increased number of cambial cells and layers compared with Col-0 control plants (left). Microscope images of transverse sections are shown at the first silique stage. Lower images show magnified images of the individual vascular bundles marked in upper images, respectively. p: phloem, pc: procambium, mx: metaxylem, px: protoxylem. Bars = 100 μm. **(B, C)** The number of cambial cells in *35S::ICA* is significantly increased compared with that in Col-0 plants **(B)**, but the cell size is not **(C)**. Cell size in each vascular tissue was measured using light microscopy and ImageJ software. Asterisk denotes statistically significant differences from Col-0 analyzed using a Student's *t* test ($^{**}P < 0.01$). Error bars indicate SE ($n \geq 9$). **(D)** The number of vascular bundles are increased in *35S::ICA* compared with Col-0. Asterisk denotes statistically significant differences from Col-0 analyzed using a Student's *t*-test ($^{**}P < 0.01$). Error bars indicate SE ($n \geq 9$). **(E, F)** *35S::ICA* shows increased stem diameter compared with Col-0 throughout the whole plant life cycle **(F)**, with a 30% increase at the first silique stage **(E)**. Asterisks denote statistically significant differences from Col-0 analyzed using a Student's *t*-test ($^{***}P < 0.001$). Error bars indicate *SE* ($n \geq 9$). All experiments were performed at least three times using biologically independent samples.

Eriksson et al. 2006), was significantly higher in *35S::ICA*, particularly vegetative internodes and cauline leaves, than in Col-0 (Figure 4B). Consistently, GA-inducible genes, such as *EXP1* (Yamauchi et al. 2004), *GASA4*, and *GASA6* (Roxrud et al. 2007; Lin et al. 2011) were upregulated in *35S::ICA* (Figure 4C). To investigate the effect of increased GA levels in *35S::ICA* on inflorescence stem development, plants were treated with paclobutrazol (PAC), a GA biosynthesis inhibitor. The lengths of vegetative internodes and the inflorescence stem were decreased in both *35S::ICA* and Col-0 on PAC treatment, but *35S::ICA* still showed the increased traits compared to Col-0 regardless of PAC application (Figure 4D, E). Whereas, the diameters of stems were not affected (Figure 4F). These results suggest that elevated GAs in *35S::ICA* contribute to stem elongation but not to radial thickening in the inflorescence stem. Interestingly, active indole acetic acid (IAA) levels were declined in rosette and cauline leaves of *35S::ICA* but increased in the main stem, especially in vegetative internodes (Table S2). JA levels were also increased in all tissues of *35S::ICA* except the axillary stem (Table S2).

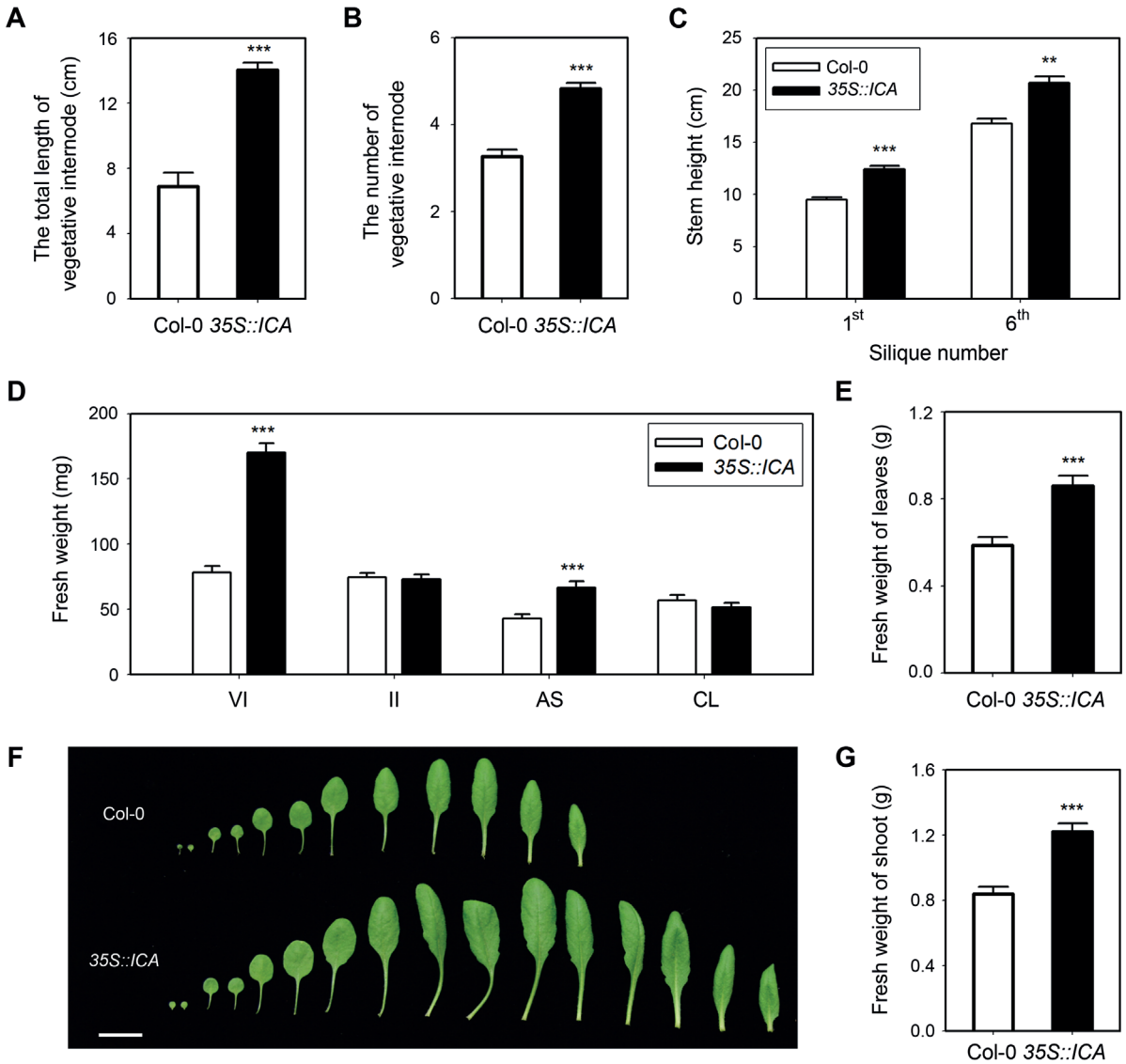

Figure 2. *35S::ICA* increases biomass production

(A) The vegetative internodes of *35S::ICA* are longer than those of Col-0 plants. The total length was measured from the ground to the first uppermost vegetative node. Asterisk denotes statistically significant differences from Col-0 analyzed using a Student's *t*-test ($^{***}P < 0.001$). Error bars indicate SE ($n = 11$). **(B)** *35S::ICA* shows increased vegetative internodes. Asterisk denotes statistically significant differences from Col-0 analyzed using a Student's *t*-test ($^{***}P < 0.001$). Error bars indicate SE ($n \geq 30$). **(C)** *35S::ICA* shows an increase in stem height. Stem height was measured at the first or sixth silique stages. Asterisks denote statistically significant differences from Col-0 analyzed using a Student's *t*-test ($^{**}P < 0.01$, $^{***}P < 0.001$). Error bars indicate SE ($n \geq 7$). **(D)** *35S::ICA* shows enhanced growth of vegetative internodes and axillary stems. AS, axillary stem; CL, cauline leaves; II, inflorescence internode; VI, vegetative internode. **(E)** The fresh weight of *35S::ICA* rosette leaves is increased compared to Col-0 at the sixth silique stage. **(F)** Leaves of *35S::ICA* are larger than those of Col-0. Representative leaves when the bolt was approximately 1 cm high are shown. Bar = 2 cm. **(G)** *35S::ICA* shows the increased biomass of shoot. **(D, E, G)** Fresh weight was measured at the sixth silique stage. Asterisks denote statistically significant differences from Col-0 analyzed using a Student's *t* test ($^{***}P < 0.001$). Error bars indicate *SE* ($n = 9$). All experiments were performed at least three times using biologically independent samples.

35S::ICA highly expresses *AT5G40830*, which encodes a putative methyltransferase

As FOX lines carry full-length cDNAs under the control of the 35S promoter in the pBIG2113SF expression vector, we identified that *35S::ICA* harbored overexpressed *At5G40830* by using vector-specific primers and confirmed that the expression of *AT5G40830* was highly and significantly increased in *35S::ICA* compared with Col-0 (Figure 5A). Therefore, *AT5G40830* is henceforth referred to as *ICA*. It was revealed that T-DNA of pBIG2113SF expression vector

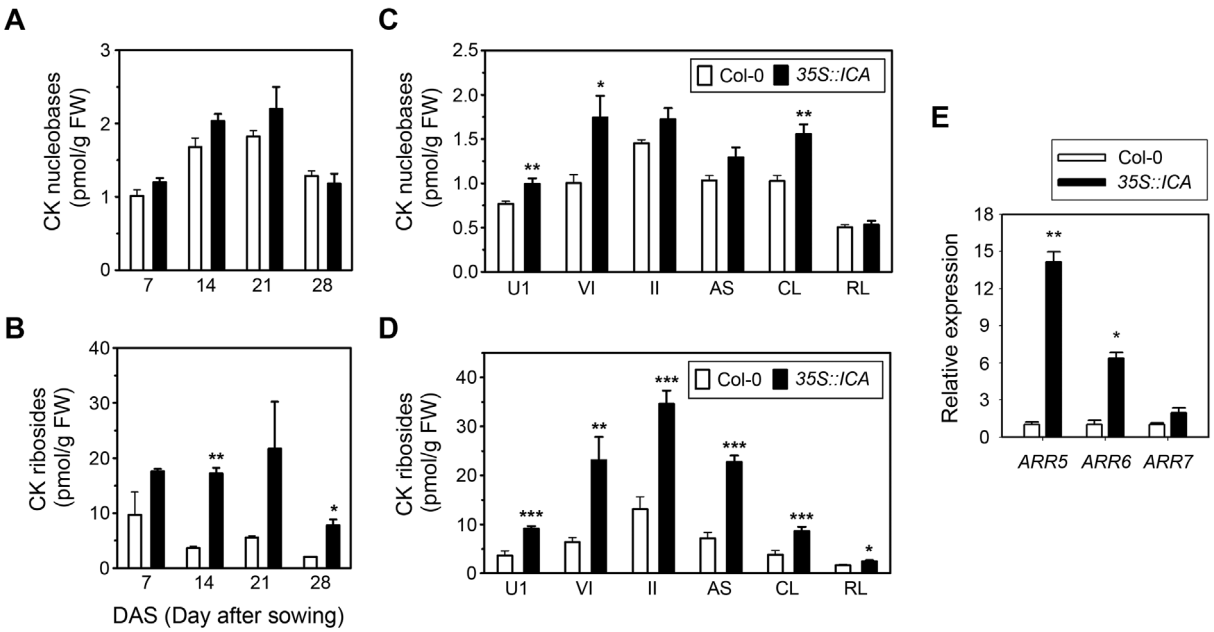

Figure 3. Cytokinin levels, especially those of CK nucleobases and ribosides, are significantly increased in *35S::ICA*
(A–D) *35S::ICA* increases the amounts of endogenous CK bases **(A, C)** and CK ribosides **(B, D)**. CK levels were measured in leaf tissues at different developmental stages **(A, B)**, and in various tissues at the sixth silique stage **(C, D)**. CK nucleobases are *trans*-zeatin (tZ), N^6-(Δ^2-isopentenyl) adenine (iP), *cis*-zeatin (cZ), and dihydrozeatin (DZ), CK ribosides are tZR, iPR, cZR, and DZR. Endogenous levels of each CK species are shown in Table S1. U1, the uppermost 1 cm tissue of the vegetative internode; VI, the other vegetative internodes except U1; II, inflorescence internode; AS, axillary stem; CL, cauline leaves; RL, rosette leaves. Asterisks denote statistically significant differences from Col-0 using a Student's *t*-test ($^*P < 0.05$, $^{**}P < 0.01$, $^{***}P < 0.001$). Error bars indicate *SE* ($n \geq 3$). **(E)** The expression of CK-responsive markers including *ARR5*, *ARR6*, and *ARR7* is increased in *35S::ICA*. Total RNA was isolated from the inflorescence stem at the sixth silique stage. *UBQ1* was used for normalization. The expression levels of each gene correspond to fold change from *35S::ICA* and Col-0 plants. Also, expression levels of each gene in Col-0 are set to 1. Asterisks denote statistically significant differences from Col-0 using a Student's *t* test ($^*P < 0.05$, $^{**}P < 0.01$). Error bars indicate *SE* ($n \geq 3$). The experiment was performed at least three times using biologically independent samples.

containing *ICA* cDNA was inserted into an intergenic region between *AT3G52670* and *AT3G52680* in chromosome 3 as confirmed by the analysis of thermal asymmetric interlaced PCR (TAIL-PCR) (Figure 5B). *ICA* encodes an SAM-dependent methyltransferase superfamily protein that has an N-terminal transmembrane domain and a putative methyltransferase domain, DUF248 (Figure 5B). To investigate spatial and temporal expression patterns of *ICA*, we generated a set of transgenic plants expressing *GUS* under the control of a approximately 2 kb *ICA* promoter. Strong *GUS* expression was observed in the entire plant vasculature of cotyledons and mature leaves (Figure 5C–E). GUS activity was also detected in the primary root cap and vascular parenchyma cells, as well as in the steles of roots (Figure 5F, G). In the inflorescence stem, *GUS* expression was restricted to procambial cells and interfascicular zones (Figure 5H, I). The abundant expression of *ICA* in the vascular tissue suggests that ICA plays a role in vascular development.

To determine the physiological function of *ICA*, we obtained a T-DNA insertion line (SALK_057412) of *AT5G40830*, *ica* (Figure S5A). The T-DNA was inserted in the 3′ of the exon, and *ICA* transcript was significantly reduced in *ica* as confirmed by qRT-PCR (Figure S5B). In *ica*, compared to Col-0, the stem diameter and height were slightly decreased at the first silique stage, but the total length and number of vegetative internode were significantly reduced (Figure S5C–E).

Increased methanol emission in *35S::ICA* is associated with increased plant growth

Interestingly, transcripts encoding pectin methylesterases (PMEs) involved in cell wall modification were altered in *35S::ICA* depending on their protein sequence similarity based on microarray analysis. In *Arabidopsis*, 66 genes have been annotated as potentially encoding PMEs clustered in four different groups based on a protein sequence (Louvet et al. 2006). In particular, *PME* genes in group 2 except for *AT5G49180*, expressed especially in flower buds (Louvet et al. 2006), were largely downregulated in *35S::ICA*, but those in group 1 were mostly upregulated (Figure 6A). Among genes in group 1, we confirmed that the expression of *PME1*, *PME44*, and *AT3G49220*, which are expressed in aerial parts such as leaves, SAM, and inflorescence stem, was highly enhanced in *35S::ICA* plants (Figure 6B). Considering that PMEs are enzymes that produce methanol via catalyzing the removal of methyl groups from the carboxyl residue of homogalacturonan (HG) methyl ester methylated by pectin methyltransferases (Figure 6C), the highly increased expression of genes encoding a putative pectin methyltransferase, ICA, and

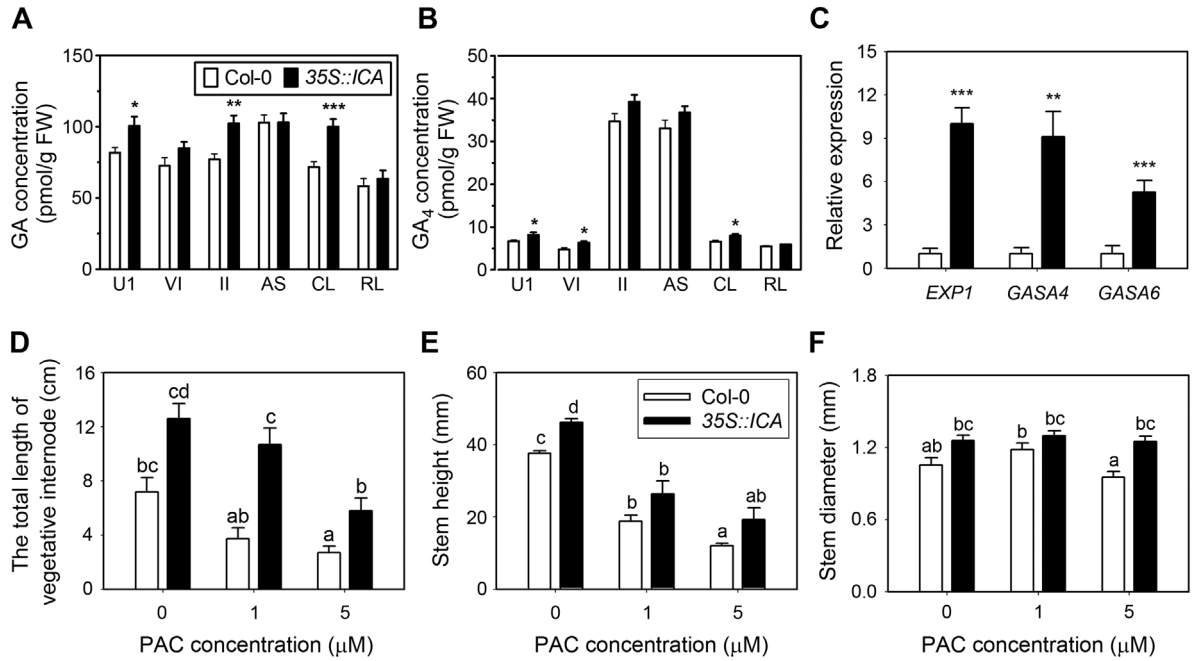

Figure 4. *35S::ICA* shows an increased level of endogenous gibberellin (GA), resulting in increased stem elongation, but not radial growth, of the inflorescence stem

(A, B) The total amount of GAs **(A)** and active GA, GA_4 **(B)**, is markedly increased in *35S::ICA*. GA levels were measured in various tissues at the sixth silique stage. Concentrations of each GA species are shown in Table S2. U1, the uppermost 1 cm tissue of vegetative internode; VI, the other vegetative internodes except U1; II, inflorescence internode; AS, axillary stem; CL, cauline leaves; RL, rosette leaves. Asterisks denote statistically significant differences from Col-0 analyzed using a Student's *t*-*test ($^{*}P < 0.05$, $^{**}P < 0.01$, $^{***}P < 0.001$). Error bars indicate SE ($n = 9$). **(C)** GA-responsive genes are upregulated in *35S::ICA*. Total RNA was isolated from the inflorescence stem at the sixth silique stage. *UBQ1* was used for normalization. The expression levels of each gene correspond to fold change from *35S::ICA* and Col-0 plants. Also, expression levels of each gene in Col-0 are set to 1. Asterisks denote statistically significant differences from Col-0 analyzed using a Student's *t* test ($^{**}P < 0.01$, $^{***}P < 0.001$). Error bars indicate *SE* ($n \geq 8$). **(D, E)** The length of *35S::ICA* vegetative internodes **(D)** and the height of the inflorescence stem **(E)** are decreased in Col-0 and *35S::ICA* in the presence of PAC, a GA synthesis inhibitor. **(F)** The stem diameter of *35S::ICA* is not affected by PAC treatment. **(D–F)** These growth characteristics were measured after plants had stopped to develop a flower in the SAM. Statistical differences were calculated using one-way ANOVA between groups ($P < 0.05$, $n = 5$). Bars with letters at the top indicate the significant difference in their phenotypes. All experiments were performed at least three times using biologically independent samples.

PMEs, suggests increased production of methanol as well as alteration of cell wall modification in *35S::ICA*. We accordingly measured the amount of methanol released through transpiration using a purpald/alcohol oxidase assay. The total emitted amount of methanol was significantly increased in *35S::ICA* compared to Col-0 in both 16- and 19-day-old seedlings even though methanol emission per leaf area was similar to each other (Figure 7A, B). Methanol increases growth and development in various plant species (Nonomura and Benson 1992; Madhaiyan et al. 2006; Ramírez et al. 2006). To determine whether or not growth phenotypic changes in *35S::ICA* could be caused by increased emission of methanol, we examined phenotypes and RNA expressions during the application of methanol in an airtight container. Increased cambial activity was observed under daily methanol treatment compared with mock treatment as control at the first silique stage (Figure 7C). In addition, daily methanol treatment significantly enhanced not only stem height but also diameter in comparison with mock treatment throughout the life cycle (Figure 7D, E) and induced the expression of *PMEs*, CK-, and GA-responsive genes at the first silique stage in the inflorescence stem (Figure 7F, G). These data suggest that the increased methanol emission in *35S::ICA* could act to stimulate growth and development in the inflorescence stem. We then tested the hypothesis that methanol functioning as a volatile organic compound affects the growth and development of neighboring plants. Col-0 plants in mixed culture with *35S::ICA* showed slightly increased stem elongation in comparison with Col-0 in monoculture, and increased radial growth was evident in Col-0 plants in mixed culture (Figure 7H, I). Surprisingly, the expression of the CK marker genes such as *ARR5*, *ARR6*, and *ARR7* was significantly increased in Col-0 plants in mixed culture compared with those in monoculture (Figure 7J). Taking all findings together, we propose that *35S::ICA* modulates the homeostasis of plant hormone levels, especially CK and GA, by the action of increased methanol, which leads to increased inflorescence stem growth.

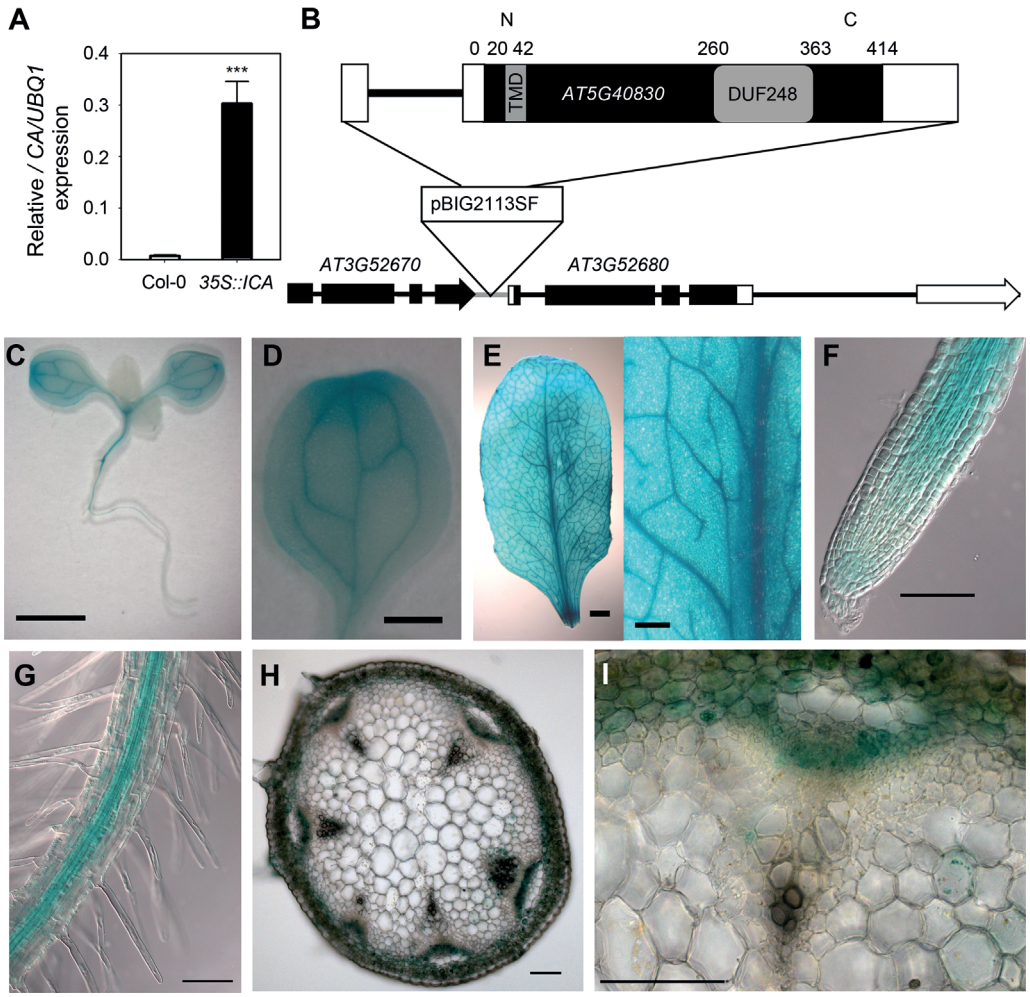

Figure 5. *35S::ICA* overexpresses the *AT5G40830* gene, which encodes a putative methyltransferase
(A) The transcript levels of *AT5G40830* are highly and specifically increased in *35S::ICA* compared with those in Col-0. Total RNA was isolated from the inflorescence stem at the sixth silique stage. *UBQ1* was used for normalization. Asterisk denotes statistically significant difference in expression ($^{***}P < 0.001$ for Student's *t*-tests). Error bars indicate SE ($n \geq 9$). The experiment was performed at least three times using biologically independent samples. **(B)** *ICA* cDNA encoding a protein which contains a transmembrane and DUF248 domain is inserted into an intergenic region between *AT3G52670* and *AT3G52680*. pBIG2113SF binary vector was used to generate the FOX lines. The black and white boxes indicate exons and UTR regions respectively in each gene. The black and gray lines indicate introns and intergenic region respectively. The arrow indicates the direction of transcription. The gray boxes within the single exon of *ICA* indicate a transmembrane domain (TMD) at the N terminus and a DUF248 domain at the C terminus predicted to function as a S-adenosyl-L-methionine (SAM)-dependent methyltransferase. The numbers indicate amino acid residues. **(C–G)** Strong GUS staining is observed in vascular tissues of the leaves, roots, and inflorescence stem of *proICA::GUS* transgenic plants. GUS expression is pronounced in veins of cotyledons **(C, D)**, steles of roots **(F, G)** in 11-day-old seedlings, and vascular tissues of leaves in 30-day-old plants **(E)**. **(H, I)** Cross-section at the base of the inflorescence stem at the first silique stage shows expression in the procambial cells and interfascicular zones in the vasculature. Bars: **(C, E left)** 2 cm; **(D, E right)** 500 μm; **(F–I)** 100 μm.

DISCUSSION

This study identified that a new putative pectin methyltransferase, ICA, can be involved in the regulation of methanol production, hormone homeostasis, cambial activity, and plant growth.

ICA has a putative SAM-dependent methyltransferase region within DUF248 domain which shares 68.4% and 61.2% amino acid sequence similarity to those of QUA2 and QUA3, respectively. The SAM-dependent methyltransferase region of DUF248 domain in ICA also shows 55.1% amino acid sequence similarity to those in CGR2 and CGR3. QUA3, CGR2, and CGR3 biochemically mediate HG methylesterification (Held et al. 2011; Miao et al. 2011; Kim et al. 2015) and QUA2 is known to be involved in HG biosynthesis (Krupková et al. 2007; Mouille et al. 2007); therefore, with high sequence similarity of the pectin methyltransferase domain, it is possible that ICA

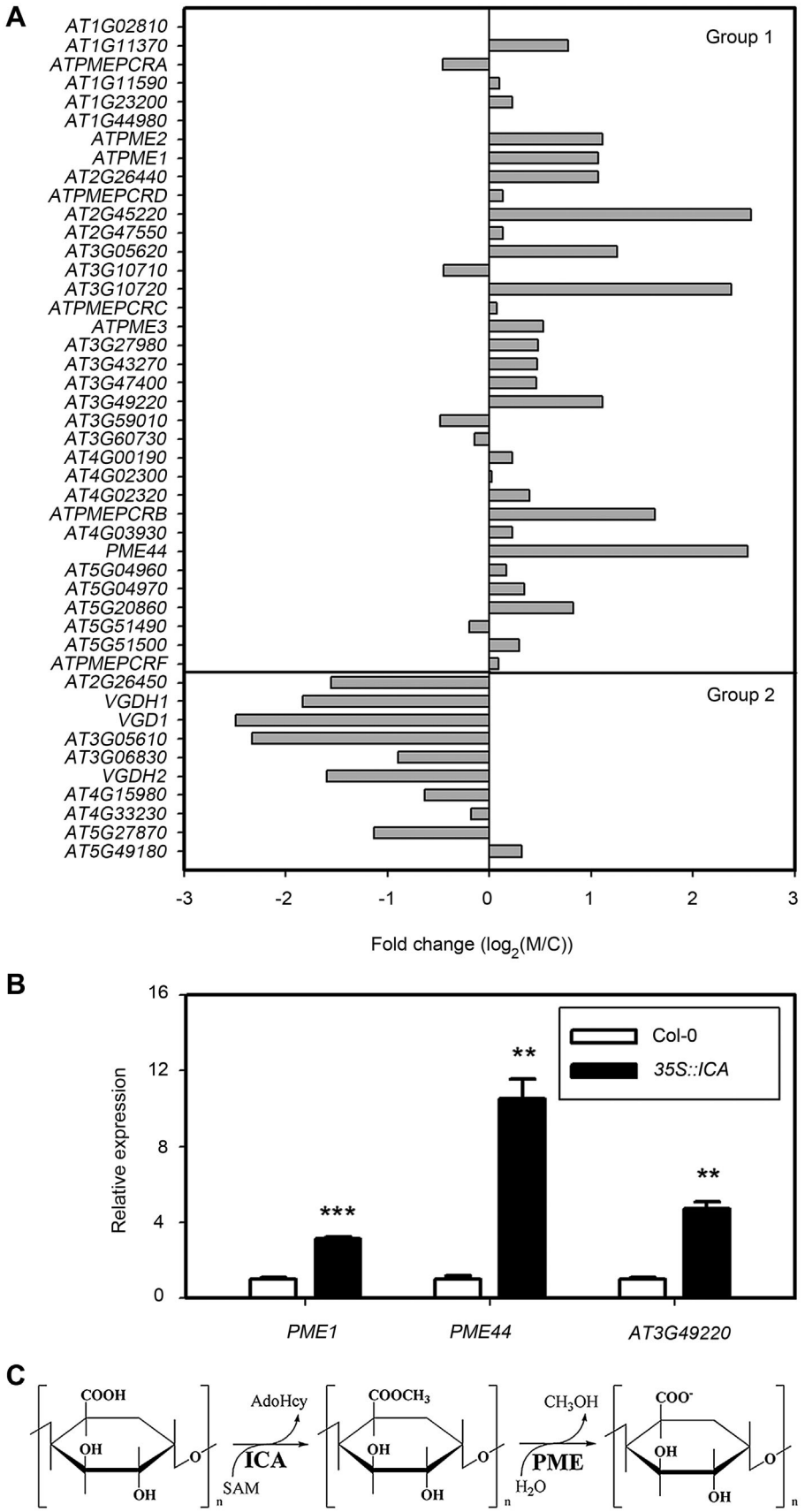

Figure 6. Continued.

also contributes to HG modification. In addition, similar to phenotypes of *35S::ICA*, ectopic expression of *CGR2* or *CGR3* increased leaf size, petiole length, and fresh weight in rosette leaves (Held et al. 2011; Kim et al. 2015) and *QUA2* and its closest homologs, *QUASIMODO2 LIKE1 (QUL1)* and *QUL2*, were involved in the vascular development of the inflorescence stem (Fuentes et al. 2010).

Highly methylated HG, which could be also affected by a putative methyltransferase ICA in pectin modification, is known to increase the activity of PMEs (Guénin et al. 2011). Methanol is mainly produced by demethylation of pectin such as HG in the cell wall through the action of PMEs (Pelloux et al. 2007; Jolie et al. 2010). Therefore, it is possible that increased expression of *ICA* may enhance the degree of HG methylation, which leads to increased PME activity, and eventually methanol emission. Considering that foliar treatment with methanol promotes stem elongation and biomass accumulation in *Arabidopsis* (Ramírez et al. 2006), and the repeated application of low quantity of methanol increases plant growth similar to a single apllication of high dosage of methanol (Nonomura and Benson 1992), the increase of total amount in methanol emission could be related to plant growth and development in *35S::ICA*. We also found that exogenous methanol enhanced radial growth as well as stem elongation in the inflorescence stem and accelerated vascular development as that observed in phenotypes of *35S::ICA* with increased levels of emitted methanol (Figure 7). Methanol is known to induce the expression of certain *PMEs* (Ramírez et al. 2006) as observed in this study (Figure 7). As the upregulated expression of *PMEs* could be linked to increase methanol emission (Dorokhov et al. 2012; Dixit et al. 2013), we hypothesize that this positive feedback regulation can contribute to maintain high *PME* expression and methanol emission in *35S::ICA*. Interestingly, we observed increased stem elongation and radial thickening of inflorescence stems in Col-0 co-cultured with *35S::ICA* compared with monocultured Col-0 (Figure 7). Because methanol is emitted through the stomata on the leaf as a volatile organic compound (VOC) (Nemecek-Marshall et al. 1995; Hüve et al. 2007), it is possible that methanol affects neighboring plants as well as the methanol-producing plant itself. High PME activity induced by pathogen challenge releases more methanol, leading to increased pathogen resistance in the plant being attacked and eventually in neighboring plants (Peñuelas et al. 2005; Körner et al. 2009; Dorokhov et al. 2012; Dixit et al. 2013). It is also plausible that methanol can act as a signaling molecule for the detection of growing plants nearby as methanol emission is closely dependent on the growth rate of leaves (MacDonald and Fall 1993; Hüve et al. 2007). In any case, it is likely that methanol is not only a byproduct of pectin modification but also has a distinct role in plant growth and development.

Methanol itself also can be metabolized into CO_2 (Cossins 1964), and high CO_2 concentration can increase the accumulation of glucose as well as that of sucrose and starch, promoting plant growth (Hachiya et al. 2014). Glucose induces the expression of genes involved in CK biosynthesis, metabolism, and signaling (Kushwah and Laxmi 2014). Considering that CKs, especially CK nucleobases and CK ribosides, were highly retained in *35S::ICA* during all measured developmental stages, they could be a major regulator of *35S::ICA* development mediated by methanol (Figure 3; Table S1). It is known that CK nucleobases are active forms which directly bind to AHK2, 3, and 4 receptors (Hothorn et al. 2011; Lomin et al. 2015), and CK ribosides also activates *pARR5::GUS* reporter expression but relatively lower than tZ (Spíchal et al. 2004). Endogenous levels of CK nucleobases in *35S::ICA* were not significantly increased at vegetative stages, but their high binding affinity could affect the vegetative growth of *35S::ICA*. Furthermore, the CK receptor and ARABIDOPSIS HISTIDINE-CONTAINING PHOSPHOTRANSMITTER (AHP) function in vegetative growth by regulating leaf expansion (Riefler et al. 2006; Deng et al. 2010) and Col-0 co-cultured with *35S::ICA*, similar to *35S::ICA*, showed upregulation of CK-responsive genes (Figure 7). Therefore, the increased CK levels are also likely to affect shoot growth in *35S::ICA* during the vegetative stage. Considering that CK also regulates cambial activity and vascular development (Matsumoto-Kitano et al. 2008; Nieminen et al. 2008; Hejátko et al. 2009), it is therefore possible that increased CK concentration in *35S::ICA* shoots is related to the proliferation and/or maintenance of vascular cambial cells in *35S::ICA* (McKenzie et al. 1998; Nishimura et al. 2004; Matsumoto-Kitano et al. 2008; Bartrina et al. 2011; Kiba et al. 2013). High levels of tZ-type CK predominantly regulate shoot growth and development (Kiba et al. 2013), which was similarly observed in *35S::ICA*. The increased levels of total CK in *35S::ICA* plants may be attributed to both biosynthesis and translocation of CK types. Taking these findings together, we propose that methanol could indirectly modulate CK homeostasis via its transition into photoassimilates during the early vegetative stage.

Interestingly, CK regulates genes involved in the biosynthesis of GA and IAA, affecting their levels (Ding et al. 2013). Consistently, transcriptome analysis revealed that *GA20ox1*,

Figure 6. The expression of genes encoding pectin methylesterase (PME) is altered in *35S::ICA* depending on their protein sequence similarity

(A) Genes encoding PMEs in group 1 are mostly upregulated but those in group 2 are downregulated in *35S::ICA* based on microarray analysis. Values (fold change) correspond to the $\log_2$ ratio of expression from *35S::ICA* (M) and Col-0 (C) *Arabidopsis* plants. **(B)** The expression of *PMEs* predominantly expressed in the shoot in group 1 is increased in *35S::ICA*, as confirmed using qRT-PCR. Total RNA was isolated from the inflorescence stem at the sixth silique stage. *UBQ1* was used for normalization. The expression levels of each gene correspond to fold change from *35S::ICA* and Col-0 plants. Also, expression levels of each gene in Col-0 are set to 1. Asterisks denote statistically significant differences from Col-0 using a Student's *t* test ($^{**}P < 0.01$, $^{***}P < 0.001$). Error bars indicate *SE* ($n = 3$). The experiment was performed at least three times using biologically independent samples. **(C)** Methanol is released by methyl and demethyl-esterification of homogalacturonan by pectin methyltransferases (e.g. ICA) and pectin methylesterases (PMEs).

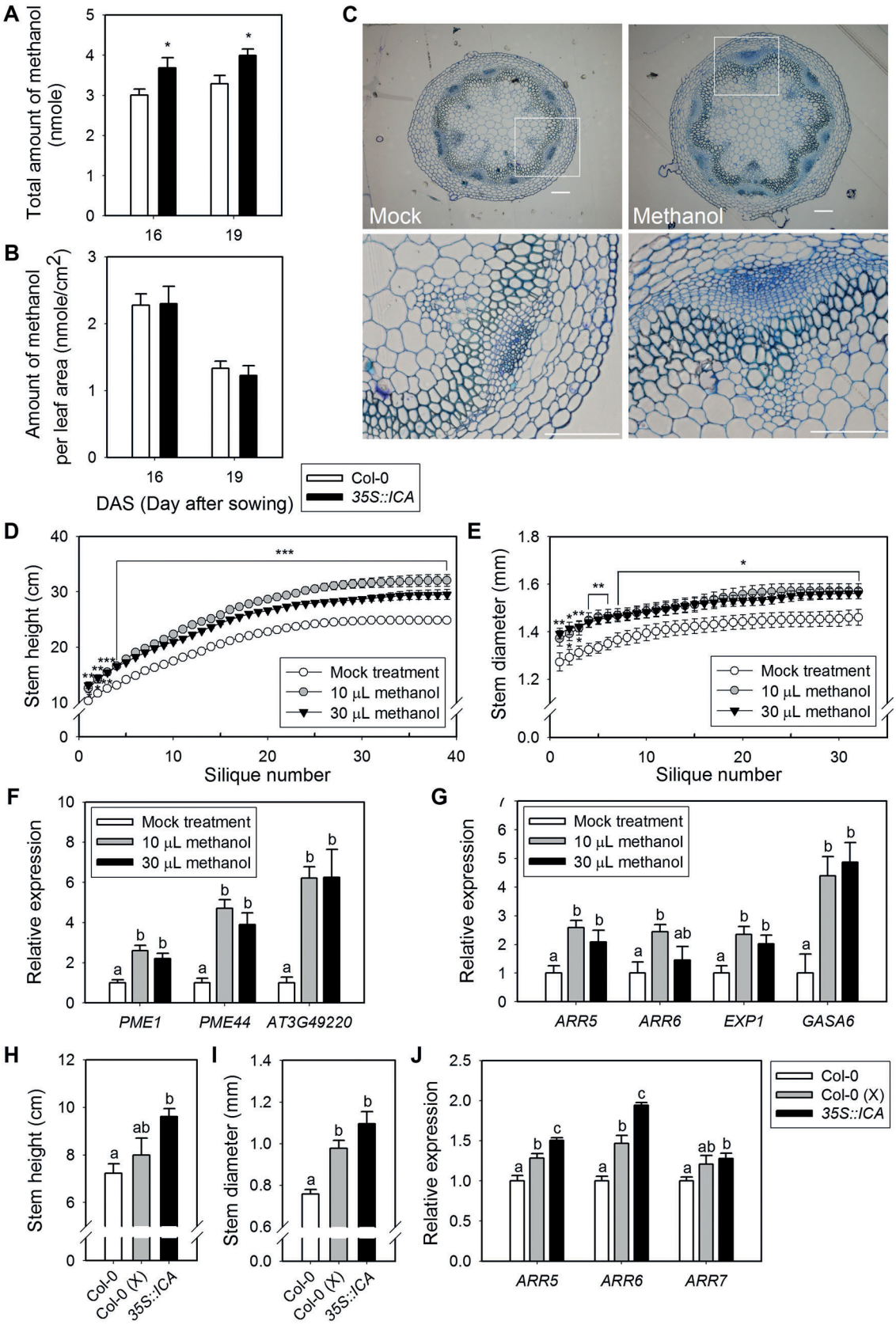

Figure 7. Continued.

which is involved in GA biosynthesis and expressed especially in the inflorescence stem (Rieu et al. 2008), was highly upregulated in *35S::ICA*. Methanol treatment also induced the expression of CK- and GA-responsive genes, similarly to its effect in *35S::ICA* (Figure 7), suggesting that growth stimulation by methanol produced in *35S::ICA* might depend on the accumulation of CKs and GAs. Interestingly, regardless of relatively low increase of bioactive GA_4 level in *35S::ICA*, GA-responsive gene expression was highly induced (Figure 4). This might be another case of nonlinear correlation between hormone content and gene expression observed in other hormone studies (Ogawa et al. 2003; Werner et al. 2003). Our study also showed that treatment of a GA synthesis inhibitor still remained longer vegetative internodes and main stem in *35S::ICA* than Col-0, which were similar to those of Col-0 without the inhibitor (Figure 4). Moreover, the expression of certain genes can be affected by several hormones simultaneously such as *EXP1* induced by both CK and GA (Ogawa et al. 2003; Bhargava et al. 2013). Therefore, we postulate that the mild increase of GA_4 could significantly affect GA responses in *35S::ICA* in which the induction of hormone-responsive genes is critical to the relative increase of hormone levels. We also found that not only CKs and GAs but also IAA and JA levels were increased in the inflorescence stem of *35S::ICA* (Table S2), probably owing to the regulation of genes involved in IAA polar transport and JA biosynthesis, as shown by the microarray analysis. IAA and JA are involved in the development of interfascicular cambium (Sehr et al. 2010; Agusti et al. 2011). The increased activity of vascular cambium in *35S::ICA* could be related to the systemic regulation of various hormones, leading to the increased biomass of the inflorescence, although it is still unclear how methanol regulates phytohormone homeostasis. The hormone homeostasis, including CK, GA, IAA, and JA, can be affected by methanol, suggesting that methanol may play distinct roles in the perception of extrinsic cues, such as the growth rate of neighboring plants, and their integration into the developmental program.

MATERIALS AND METHODS

Plant material and growth conditions

Arabidopsis thaliana ecotype Col-0 served as the wild type. The FOX line collection in *Arabidopsis* (Ichikawa et al. 2006) was used for the screening of novel regulators of vasculature. The transgene in the selected FOX line was identified by PCR of genomic DNA using a primer pair (GS4, 5′-ACATTCTACAACTACATCTAGAGG-3′, and GS6, 5′-CGGCCGCCCCGGGGATC-3′) and sequencing. The insertion site of the pBIG2113SF expression vector in FOX lines was identified by TAIL-PCR of genomic DNA as previously described (Liu et al. 1995). Three vector specific primers (LB1, 5′- CTGAATGGCGCCCGCTCC-3′, LB2, 5′-TGGTTCACGTAGTGGGCCATCG-3′, and LB3, 5′-ATTTTGCCGATTTCGGAAC-3′) and eight arbitrary degenerate (AD) primers (AD1, 5′-NTCAGSTWTSGWGWT-3′, AD2, 5′-WTGCCWNNCCCC-3′, AD3, 5′-GWSIDRAMSCTGCTC-3′, AD4, 5′-WGTGNAGWANCANAGA-3′, AD5, 5′-TTGIAGNACIANAGG-3′, AD6, 5′-AGWGNAGWANCANAGA-3′, AD7, 5′-WGCNAGTNAGWANAA-3′, AD8, 5′-AWGCANGNCWGANATA-3′) were used to perform TAIL-PCR. Seeds were germinated on 1/2 B5 medium containing 1% sucrose and 0.8% w/v agar under fluorescent light (16-h light/8-h dark) at 23 °C. Young seedlings were then transferred to soil and grown until the experiment. Seedlings grown in mixed culture using a two-compartment Petri plate (I-plate) in the media were transferred to the soil in a checked pattern. The *ica* (SALK_057412) was obtained from Arabidopsis Biological Resource Center.

Histological analysis of vasculature development

Histological analysis in the inflorescence stem was performed as previously described (Hejátko et al. 2009), with slight modifications. Inflorescence stem sections were cut from the base up to 5 mm at the stage of the first silique development. The cut samples were fixed for 3 h in 0.1 M phosphate buffer (pH 7.2) with 3% glutaraldehyde and then washed twice with the buffer alone. The fixed samples were dehydrated in graded acetone. Prepared samples were embedded in Spurr's

Figure 7. The amount of methanol is increased in *35S::ICA*, leading to stimulation of the growth of the inflorescence stem
(A, B) *35S::ICA* increases total released amount of methanol **(A)** but not methanol emission per leaf area **(B)** compared with Col-0. The emitted amount of methanol was quantified using the water released mainly by transpiration from the surface of leaves. Leaf area was measured using imageJ software. Asterisks denote statistically significant differences from Col-0 using a Student's *t*-test ($^{*}P < 0.05$). Error bars indicate *SE* ($n = 5$). **(C)** Methanol treatment (right) increases vascular tissues, especially cambial cell layers compared with mock treatment (left). Microscope images of transverse sections are shown at the first silique stage. Lower images show magnified images of the individual vascular bundles marked in upper images, respectively. Bars = 100 μm. **(D, E)** Methanol treatment increases the stem height **(D)** as well as the stem diameter **(E)**. Stem height and diameter were measured daily throughout the whole life of Col-0 and *35S::ICA* plants treated with 0 (mock control), 10, and 30 μL of 100% methanol. Asterisks denote statistically significant differences from Col-0 using a Student's *t* test ($^{*}P < 0.05$, $^{**}P < 0.01$, $^{***}P < 0.001$). Error bars indicate *SE* ($n = 8$). **(F, G)** Methanol induces the expression of *PMEs* **(F)** and CK- or GA-responsive genes **(G)**. Total RNA was isolated from inflorescence stems at the first silique stage after daily methanol treatment. *UBQ1* was used for normalization. The expression levels of each gene correspond to fold change from mock and methanol treatment. Also, expression levels of each gene in mock treatment are set to 1. Error bars indicate *SE* ($n \geq 6$). **(H, I)** Col-0 co-cultured with *35S::ICA* [Col-0 (X); mixed culture] displays increased stem elongation **(H)** and radial growth **(I)** of the inflorescence stem compared with Col-0 plants grown with themselves (monoculture). Stem height and diameter were measured at the sixth silique stage. Error bars indicate *SE* ($n \geq 5$). **(J)** The CK marker genes *ARR5*, *ARR6*, and *ARR7* are upregulated in Col-0 co-cultured with *35S::ICA* [Col-0 (X); mixed–culture]. Total RNA was isolated from 8-day-old seedlings. *UBQ1* was used for normalization. Error bars indicate *SE* ($n \geq 5$). **(F–J)** Statistical differences were calculated using one-way ANOVA between groups ($P < 0.05$). Bars with letters at the top indicate significant differences in their expressions or phenotypes. All experiments were performed at least three times using biologically independent samples.

resin for 48 h at 65 °C. Sectioned specimens (2 μm) were cut using a fully automated rotary microtome (Leica, http://www.leicabiosystems.com/), stained in 0.05% toluidine blue, and then monitored and recorded vasculature development using a Zeiss Axioplan2 microscope. Stem diameter was measured by microscopy at the stage of the first silique development and using a caliper during the whole plant life cycle. ImageJ was used for determining cell number and size in the vascular tissue.

Analysis of RAM activity and primary root growth

Plants were grown vertically in the Petri dish to measure the length of primary roots. To determine the size of meristemic zone in the root, whole-mount preparation was performed as previously described (Malamy and Benfey 1997). Length and cell number of meristemic zones, diameter, and length of 6-day-old roots were analyzed by using a Zeiss Axioplan2 microscope equipped with differential interferential contrast optics.

Exogenous methanol and paclobutrazol (PAC) treatment

Starting with 10-day-old seedlings, plants were treated with different amount of methanol for 12 h daily in an airtight container made of acrylic panel. For methanol treatment, a 1.5 mL e-tube which contains 10 or 30 μL of 100% methanol was surrounded by eight plants grown in the same container. The lid of methanol loaded e-tube was opened and tightly covered with 3 M Micropore tape (TM1530-1, http://www.3m.com/3M/en_US/company-us/) for slow volatilization during 12 h treatment daily. Final concentration of methanol within the air of container was about 0.1 and 0.3 ppm, respectively. Col-0 and *35S::ICA* plants were sprayed with 0, 1, and 5 μM PAC from 14 d after sowing at intervals of 5 d. Lengths of vegetative internodes, stem height, and diameter were recorded after plants had stopped developing flowers in the SAM.

Histochemical GUS analysis

Approximately 2.0 kb upstream sequence from the start codon of *ICA* was amplified by PCR and cloned into the pCAMBIA1303 expression vector to observe *ICA* expression pattern in planta. Transgenic plants expressing *proICA::GUS* reporter construct were generated using floral dip method mediated by *Agrobacterium tumefaciens* as described (Clough and Bent 1998; Logemann et al. 2006). T3 homozygous plants at various developmental stages were stained using X-Gluc (GOLD BIOTECHNOLOGY, http://www.goldbio.com/). For the detection of GUS staining in vascular tissues of the inflorescence stem, segments were cut using a razor blade from the bases of inflorescence stems at the stage of the first silique development. Segments were mounted in 50% glycerol and monitored and recorded using a Zeiss Axioplan2 microscope.

Microarray analysis

For microarray experiments, total RNA was isolated from the inflorescence stem at the stage of the sixth silique development in Col-0 and *35S::ICA* using TRIZOL reagent (Thermo Fisher scientific, http://www.thermofisher.com/) according to the manufacturer's instructions. RNA samples were freed of DNA contamination using DNAfree (Ambion, http://www.invitorgen.com/ambion). cDNA was synthesized using the ImProm-II reverse transcription system (Promega, http://www.promega.com/). Two biological replicates were prepared under the same growth conditions. The integrity of RNA was checked using bioanalyzer (Agilent Technologies, http://www.agilent.com/). Subsequent steps of the microarray experiment followed Agilent protocols. The microarray data performed in this paper have been deposited in the National Center for Biotechnology Information Gene Expression Omnibus database (GSE78134).

Quantitative RT-PCR analysis

Total RNA was isolated from the inflorescence stem at the stage of the first or sixth silique development and from mature leaves (aerial parts of 21-day-old seedlings) using TRIZOL reagent (Thermo Fisher scientific) according to the manufacturer's instructions. Quantitative real-time PCR was performed using SYBR Premix EX taq (Takara, http://www.takara-bio.com/) in a LightCycler 2.0 (Roche, http://www.roche.com/) using gene-specific primers. The expression levels of *UBQ1* were used as an internal control. Significant differences in transcript levels measured using qRT-PCR were identified with Student's *t*-test and ANOVA at a significance level of $P < 0.05$.

Quantification of methanol emission

Emitted amounts of methanol were measured as previously described (Dixit et al. 2013) with minor modifications. Plants (16- or 19-day-old) were individually incubated in hermetically sealed glass jars for 5 h under fluorescent light. Water on the wall was collected using a cell scraper. It was used to quantify methanol by indirect detection assay (purpald/alcohol oxidase method) as previously described (Anthon and Barrett 2004). The experiment was performed using at least three biological replicates; representative data are shown.

Quantification of endogenous hormone levels

Frozen tissues (approximately 100 mg fresh weight) of rosette leaves in 7-, 14-, 21-, and 28-day-old plants or various aerial parts at the sixth silique stage were ground to fine powder using a Mixer Mill (MM301; Retsch, http://retsch.com) with a zirconia bead and lyophilized. Extraction and determination of hormone levels were performed using ultra-performance liquid chromatography–tandem mass spectrometry as previously described (Kojima et al. 2009).

ACKNOWLEDGEMENTS

This work was carried out with the support of "Cooperative Research Program for Agriculture Science & Technology Development (Project No. PJ010953022016)" Rural Development Administration, Korea.

AUTHOR CONTRIBUTIONS

H.K. designed and performed the experiments and wrote the manuscript. M.K. and H.S. performed experiment of hormone analysis. D.C. performed microarray analysis. S.P. conceived and designed the experiment. M.M. provided FOX line collection. I.H. designed the study and wrote the manuscript.

REFERENCES

Agusti J, Herold S, Schwarz M, Sanchez P, Ljung K, Dun EA, Brewer PB, Beveridge CA, Sieberer T, Sehr EM, Greb T (2011) Strigolactone signaling is required for auxin-dependent stimulation of secondary growth in plants. **Proc Natl Acad Sci USA** 108: 20242–20247

Anthon GE, Barrett DM (2004) Comparison of three colorimetric reagents in the determination of methanol with alcohol oxidase. Application to the assay of pectin methylesterase. **J Agric Food Chem** 52: 3749–3753

Bartrina I, Otto E, Strnad M, Werner T, Schmülling T (2011) Cytokinin regulates the activity of reproductive meristems, flower organ size, ovule formation, and thus seed yield in *Arabidopsis thaliana*. **Plant Cell** 23: 69–80

Baucher M, El Jaziri M, Vandeputte O (2007) From primary to secondary growth: Arigin and development of the vascular system. **J Exp Bot** 58: 3485–3501

Bhargava A, Clabaugh I, To JP, Maxwell BB, Chiang YH, Schaller GE, Loraine A, Kieber JJ (2013) Identification of cytokinin-responsive genes using microarray meta-analysis and RNA-seq in *Arabidopsis*. **Plant Physiol** 162: 272–294

Caño-Delgado A, Lee JY, Demura T (2010) Regulatory mechanisms for specification and patterning of plant vascular tissues. **Annu Rev Cell Dev Biol** 26: 605–637

Clough SJ, Bent AF (1998) Floral dip: A simplified method for *Agrobacterium*-mediated transformation of *Arabidopsis thaliana*. **Plant J** 16: 735–743

Cossins EA (1964) The utilization of carbon-1 compounds by plants: I. The metabolism of methanol-C^{14} and its role in amino acid biosynthesis. **Can J Biochem** 42: 1793–1802

Dayan J, Voronin N, Gong F, Sun T-p, Hedden P, Fromm H, Aloni R (2012) Leaf-induced gibberellin signaling is essential for internode elongation, cambial activity, and fiber differentiation in tobacco stems. **Plant Cell** 24: 66–79

Deng Y, Dong H, Mu J, Ren B, Zheng B, Ji Z, Yang W-C, Liang Y, Zuo J (2010) *Arabidopsis* histidine kinase CKI1 acts upstream of HISTIDINE PHOSPHOTRANSFER PROTEINS to regulate female gametophyte development and vegetative growth. **Plant Cell** 22: 1232–1248

Ding J, Chen B, Xia X, Mao W, Shi K, Zhou Y, Yu J (2013) Cytokinin-induced parthenocarpic fruit development in tomato is partly dependent on enhanced gibberellin and auxin biosynthesis. **PLoS ONE** 8: e70080

Dixit S, Upadhyay SK, Singh H, Sidhu OP, Verma PC, K C (2013) Enhanced methanol production in plants provides broad spectrum insect resistance. **PLoS ONE** 8: e79664

Dorokhov YL, Komarova TV, Petrunia IV, Frolova OY, Pozdyshev DV, Gleba YY (2012) Airborne signals from a wounded leaf facilitate viral spreading and induce antibacterial resistance in neighboring plants. **PLoS Pathog** 8: e1002640

Druart N, Johansson A, Baba K, Schrader J, Sjödin A, Bhalerao RR, Resman L, Trygg J, Moritz T, Bhalerao RP (2007) Environmental and hormonal regulation of the activity–dormancy cycle in the cambial meristem involves stage-specific modulation of transcriptional and metabolic networks. **Plant J** 50: 557–573

Elo A, Immanen J, Nieminen K, Helariutta Y (2009) Stem cell function during plant vascular development. **Semin Cell Dev Biol** 20: 1097–1106

Eriksson ME, Israelsson M, Olsson O, Moritz T (2000) Increased gibberellin biosynthesis in transgenic trees promotes growth, biomass production and xylem fiber length. **Nat Biotechnol** 18: 784–788

Eriksson S, Böhlenius H, Moritz T, Nilsson O (2006) GA_4 is the active gibberellin in the regulation of *LEAFY* transcription and *Arabidopsis* floral initiation. **Plant Cell** 18: 2172–2181

Etchells JP, Mishra Laxmi S, Kumar M, Campbell L, Turner Simon R (2015) Wood formation in trees is increased by manipulating PXY-regulated cell division. **Curr Biol** 25: 1050–1055

Etchells JP, Provost CM, Mishra L, Turner SR (2013) *WOX4* and *WOX14* act downstream of the PXY receptor kinase to regulate plant vascular proliferation independently of any role in vascular organisation. **Development** 140: 2224–2234

Fisher K, Turner S (2007) PXY, a receptor-like kinase essential for maintaining polarity during plant vascular-tissue development. **Curr Biol** 17: 1061–1066

Fuentes S, Pires N, Østergaard L (2010) A clade in the *QUASIMODO2* family evolved with vascular plants and supports a role for cell wall composition in adaptation to environmental changes. **Plant Mol Biol** 73: 605–615

Funada R, Miura T, Shimizu Y, Kinase T, Nakaba S, Kubo T, Sano Y (2008) Gibberellin-induced formation of tension wood in angiosperm trees. **Planta** 227: 1409–1414

Guénin S, Mareck A, Rayon C, Lamour R, Assoumou Ndong Y, Domon J-M, Sénéchal F, Fournet F, Jamet E, Canut H, Percoco G, Mouille G, Rolland A, Rustérucci C, Guerineau F, Van Wuytswinkel O, Gillet F, Driouich A, Lerouge P, Gutierrez L, Pelloux J (2011) Identification of pectin methylesterase 3 as a basic pectin methylesterase isoform involved in adventitious rooting in *Arabidopsis thaliana*. **New Phytol** 192: 114–126

Hüve K, Christ M, Kleist E, Uerlings R, Niinemets Ü, Walter A, Wildt J (2007) Simultaneous growth and emission measurements demonstrate an interactive control of methanol release by leaf expansion and stomata. **J Exp Bot** 58: 1783–1793

Hachiya T, Sugiura D, Kojima M, Sato S, Yanagisawa S, Sakakibara H, Terashima I, Noguchi K (2014) High CO_2 triggers preferential root growth of *Arabidopsis thaliana* via two distinct systems under low pH and low N stresses. **Plant Cell Physiol** 55: 269–280

Hejátko J, Ryu H, Kim G-T, Dobešová R, Choi S, Choi SM, Souček P, Horák J, Pekárová B, Palme K, Brzobohatý B, Hwang I (2009) The histidine kinases CYTOKININ-INDEPENDENT1 and ARABIDOPSIS HISTIDINE KINASE2 and 3 regulate vascular tissue development in *Arabidopsis* shoots. **Plant Cell** 21: 2008–2021

Held MA, Be E, Zemelis S, Withers S, Wilkerson C, Brandizzi F (2011) CGR3: a Golgi-localized protein influencing homogalacturonan methylesterification. **Mol Plant** 4: 832–844

Hirakawa Y, Kondo Y, Fukuda H (2010) TDIF peptide signaling regulates vascular stem cell proliferation via the *WOX4* homeobox gene in *Arabidopsis*. **Plant Cell** 22: 2618–2629

Hirakawa Y, Shinohara H, Kondo Y, Inoue A, Nakanomyo I, Ogawa M, Sawa S, Ohashi-Ito K, Matsubayashi Y, Fukuda H (2008) Non-cell-autonomous control of vascular stem cell fate by a CLE peptide/receptor system. **Proc Natl Acad Sci USA** 105: 15208–15213

Hirose N, Makita N, Yamaya T, Sakakibara H (2005) Functional characterization and expression analysis of a gene, *OsENT2*, encoding an equilibrative nucleoside transporter in rice suggest a function in cytokinin transport. **Plant Physiol** 138: 196–206

Hothorn M, Dabi T, Chory J (2011) Structural basis for cytokinin recognition by *Arabidopsis thaliana* histidine kinase 4. **Nat Chem Biol** 7: 766–768

Ichikawa T, Nakazawa M, Kawashima M, Iizumi H, Kuroda H, Kondou Y, Tsuhara Y, Suzuki K, Ishikawa A, Seki M, Fujita M, Motohashi R, Nagata N, Takagi T, Shinozaki K, Matsui M (2006) The FOX hunting system: An alternative gain-of-function gene hunting technique. **Plant J** 48: 974–985

Ilegems M, Douet V, Meylan-Bettex M, Uyttewaal M, Brand L, Bowman JL, Stieger PA (2010) Interplay of auxin, KANADI and Class III HD-ZIP transcription factors in vascular tissue formation. **Development** 137: 975–984

Israelsson M, Sundberg B, Moritz T (2005) Tissue-specific localization of gibberellins and expression of gibberellin-biosynthetic and signaling genes in wood-forming tissues in aspen. **Plant J** 44: 494–504

Jolie RP, Duvetter T, Van Loey AM, Hendrickx ME (2010) Pectin methylesterase and its proteinaceous inhibitor: A review. **Carbohydr Res** 345: 2583–2595

Körner E, von Dahl CC, Bonaventure G, Baldwin IT (2009) Pectin methylesterase Na*PME1* contributes to the emission of methanol during insect herbivory and to the elicitation of defence responses in *Nicotiana attenuata*. **J Exp Bot** 60: 2631–2640

Kiba T, Takei K, Kojima M, Sakakibara H (2013) Side-chain modification of cytokinins controls shoot growth in *Arabidopsis*. **Dev Cell** 27: 452–461

Kim SJ, Held MA, Zemelis S, Wilkerson C, Brandizzi F (2015) CGR2 and CGR3 have critical overlapping roles in pectin methylesterification and plant growth in *Arabidopsis thaliana*. **Plant J** 82: 208–220

Ko D, Kang J, Kiba T, Park J, Kojima M, Do J, Kim KY, Kwon M, Endler A, Song WY, Martinoia E, Sakakibara H, Lee Y (2014) *Arabidopsis* ABCG14 is essential for the root-to-shoot translocation of cytokinin. **Proc Natl Acad Sci USA** 111: 7150–7155

Ko JH, Han KH, Park S, Yang J (2004) Plant body weight-induced secondary growth in *Arabidopsis* and its transcription phenotype revealed by whole-transcriptome profiling. **Plant Physiol** 135: 1069–1083

Kojima M, Kamada-Nobusada T, Komatsu H, Takei K, Kuroha T, Mizutani M, Ashikari M, Ueguchi-Tanaka M, Matsuoka M, Suzuki K, Sakakibara H (2009) Highly sensitive and high-throughput analysis of plant hormones using MS-probe modification and liquid chromatography–tandem mass spectrometry: An application for hormone profiling in *Oryza sativa*. **Plant Cell Physiol** 50: 1201–1214

Krupková E, Immerzeel P, Pauly M, Schmülling T (2007) The *TUMOROUS SHOOT DEVELOPMENT2* gene of *Arabidopsis* encoding a putative methyltransferase is required for cell adhesion and co-ordinated plant development. **Plant J** 50: 735–750

Kushwah S, Laxmi A (2014) The interaction between glucose and cytokinin signal transduction pathway in *Arabidopsis thaliana*. **Plant Cell Environ** 37: 235–253

Lin PC, Pomeranz MC, Jikumaru Y, Kang SG, Hah C, Fujioka S, Kamiya Y, Jang JC (2011) The *Arabidopsis* tandem zinc finger protein AtTZF1 affects ABA- and GA-mediated growth, stress and gene expression responses. **Plant J** 65: 253–268

Liu YG, Mitsukawa N, Oosumi T, Whittier RF (1995) Efficient isolation and mapping of *Arabidopsis thaliana* T-DNA insert junctions by thermal asymmetric interlaced PCR. **Plant J** 8: 457–463

Logemann E, Birkenbihl RP, Ülker B, Somssich IE (2006) An improved method for preparing Agrobacterium cells that simplifies the *Arabidopsis* transformation protocol. **Plant Methods** 2: 16

Lomin SN, Krivosheev DM, Steklov MY, Arkhipov DV, Osolodkin DI, Schmülling T, Romanov GA (2015) Plant membrane assays with cytokinin receptors underpin the unique role of free cytokinin bases as biologically active ligands. **J Exp Bot** 66: 1851–1863

Louvet R, Cavel E, Gutierrez L, Guénin S, Roger D, Gillet F, Guerineau F, Pelloux J (2006) Comprehensive expression profiling of the pectin methylesterase gene family during silique development in *Arabidopsis thaliana*. **Planta** 224: 782–791

Mähönen AP, Bonke M, Kauppinen L, Riikonen M, Benfey PN, Helariutta Y (2000) A novel two-component hybrid molecule regulates vascular morphogenesis of the *Arabidopsis* root. **Genes Dev** 14: 2938–2943

MacDonald RC, Fall R (1993) Detection of substantial emissions of methanol from plants to the atmosphere. **Atmos Environ** 27: 1709–1713

Madhaiyan M, Poonguzhali S, Sundaram SP, Sa T (2006) A new insight into foliar applied methanol influencing phylloplane methylotrophic dynamics and growth promotion of cotton (*Gossypium hirsutum* L.) and sugarcane (*Saccharum officinarum* L.). **Environ Exp Bot** 57: 168–176

Malamy JE, Benfey PN (1997) Analysis of *SCARECROW* expression using a rapid system for assessing transgene expression in *Arabidopsis* roots. **Plant J** 12: 957–963

Matsumoto-Kitano M, Kusumoto T, Tarkowski P, Kinoshita-Tsujimura K, Václavíková K, Miyawaki K, Kakimoto T (2008) Cytokinins are central regulators of cambial activity. **Proc Natl Acad Sci USA** 105: 20027–20031

McKenzie MJ, Mett V, Reynolds PHS, Jameson PE (1998) Controlled cytokinin production in transgenic tobacco using a copper-inducible promoter. **Plant Physiol** 116: 969–977

Miao Y, Li H-Y, Shen J, Wang J, Jiang L (2011) QUASIMODO 3 (QUA3) is a putative homogalacturonan methyltransferase regulating cell wall biosynthesis in *Arabidopsis* suspension-cultured cells. **J Exp Bot** 62: 5063–5078

Miyashima S, Sebastian J, Lee JY, Helariutta Y (2013) Stem cell function during plant vascular development. **EMBO J** 32: 178–193

Miyawaki K, Matsumoto-Kitano M, Kakimoto T (2004) Expression of cytokinin biosynthetic isopentenyltransferase genes in *Arabidopsis*: tissue specificity and regulation by auxin, cytokinin, and nitrate. **Plant J** 37: 128–138

Mouille G, Ralet MC, Cavelier C, Eland C, Effroy D, Hématy K, McCartney L, Truong HN, Gaudon V, Thibault JF, Marchant A, Höfte H (2007) Homogalacturonan synthesis in *Arabidopsis thaliana* requires a Golgi-localized protein with a putative methyltransferase domain. **Plant J** 50: 605–614

Nemecek-Marshall M, MacDonald RC, Franzen JJ, Wojciechowski CL, Fall R (1995) Methanol emission from leaves (enzymatic detection of gas-phase methanol and relation of methanol fluxes to stomatal conductance and leaf development). **Plant Physiol** 108: 1359–1368

Nieminen K, Immanen J, Laxell M, Kauppinen L, Tarkowski P, Dolezal K, Tähtiharju S, Elo A, Decourteix M, Ljung K, Bhalerao R, Keinonen K, Albert VA, Helariutta Y (2008) Cytokinin signaling regulates cambial development in poplar. **Proc Natl Acad Sci USA** 105: 20032–20037

Nieminen K, Robischon M, Immanen J, Helariutta Y (2012) Towards optimizing wood development in bioenergy trees. **New Phytol** 194: 46–53

Nilsson J, Karlberg A, Antti H, Lopez-Vernaza M, Mellerowicz E, Perrot-Rechenmann C, Sandberg G, Bhalerao RP (2008) Dissecting the molecular basis of the regulation of wood formation by auxin in hybrid aspen. **Plant Cell** 20: 843–855

Nishimura C, Ohashi Y, Sato S, Kato T, Tabata S, Ueguchi C (2004) Histidine kinase homologs that act as cytokinin receptors possess overlapping functions in the regulation of shoot and root growth in *Arabidopsis*. **Plant Cell** 16: 1365–1377

Nonomura AM, Benson AA (1992) The path of carbon in photosynthesis: Improved crop yields with methanol. **Proc Natl Acad Sci USA** 89: 9794–9798

Ogawa M, Hanada A, Yamauchi Y, Kuwahara A, Kamiya Y, Yamaguchi S (2003) Gibberellin biosynthesis and response during *Arabidopsis* seed germination. **Plant Cell** 15: 1591–1604

Peñuelas J, Filella I, Stefanescu C, Llusià J (2005) Caterpillars of *Euphydryas aurinia* (Lepidoptera: Nymphalidae) feeding on *Succisa pratensis* leaves induce large foliar emissions of methanol. **New Phytol** 167: 851–857

Pelloux J, Rustérucci C, Mellerowicz EJ (2007) New insights into pectin methylesterase structure and function. **Trends Plant Sci** 12: 267–277

Ragni L, Nieminen K, Pacheco-Villalobos D, Sibout R, Schwechheimer C, Hardtke CS (2011) Mobile gibberellin directly stimulates *Arabidopsis* hypocotyl xylem expansion. **Plant Cell** 23: 1322–1336

Ramírez I, Dorta F, Espinoza V, Jiménez E, Mercado A, Peña-Cortés H (2006) Effects of foliar and root applications of methanol on the growth of *Arabidopsis*, tobacco, and tomato plants. **J Plant Growth Regul** 25: 30–44

Riefler M, Novak O, Strnad M, Schmülling T (2006) *Arabidopsis* cytokinin receptor mutants reveal functions in shoot growth, leaf senescence, seed size, germination, root development, and cytokinin metabolism. **Plant Cell** 18: 40–54

Rieu I, Ruiz-Rivero O, Fernandez-Garcia N, Griffiths J, Powers SJ, Gong F, Linhartova T, Eriksson S, Nilsson O, Thomas SG, Phillips AL, Hedden P (2008) The gibberellin biosynthetic genes *AtGA20ox1* and *AtGA20ox2* act, partially redundantly, to promote growth and development throughout the *Arabidopsis* life cycle. **Plant J** 53: 488–504

Roxrud I, Lid SE, Fletcher JC, Schmidt EDL, Opsahl-Sorteberg H-G (2007) GASA4, one of the 14-member *Arabidopsis* GASA family of small polypeptides, regulates flowering and seed development. **Plant Cell Physiol** 48: 471–483

Scarpella E, Meijer AH (2004) Pattern formation in the vascular system of monocot and dicot plant species. **New Phytol** 164: 209–242

Sehr EM, Agusti J, Lehner R, Farmer EE, Schwarz M, Greb T (2010) Analysis of secondary growth in the *Arabidopsis* shoot reveals a positive role of jasmonate signalling in cambium formation. **Plant J** 63: 811–822

Spíchal L, Rakova NY, Riefler M, Mizuno T, Romanov GA, Strnad M, Schmülling T (2004) Two cytokinin receptors of *Arabidopsis thaliana*, CRE1/AHK4 and AHK3, differ in their ligand specificity in a bacterial assay. **Plant Cell Physiol** 45: 1299–1305

Sponsel VM, Schmidt FW, Porter SG, Nakayama M, Kohlstruk S, Estelle M (1997) Characterization of new gibberellin-responsive semidwarf mutants of Arabidopsis. **Plant Physiol** 115: 1009–1020

Suer S, Agusti J, Sanchez P, Schwarz M, Greb T (2011) *WOX4* imparts auxin responsiveness to cambium cells in *Arabidopsis*. **Plant Cell** 23: 3247–3259

Uggla C, Mellerowicz EJ, Sundberg B (1998) Indole-3-acetic acid controls cambial growth in Scots pine by positional signaling. **Plant Physiol** 117: 113–121

Uggla C, Moritz T, Sandberg G, Sundberg B (1996) Auxin as a positional signal in pattern formation in plants. **Proc Natl Acad Sci USA** 93: 9282–9286

Werner T, Motyka V, Laucou V, Smets R, Van Onckelen H, Schmülling T (2003) Cytokinin-deficient transgenic *Arabidopsis* plants show multiple developmental alterations indicating opposite functions of cytokinins in the regulation of shoot and root meristem activity. **Plant Cell** 15: 2532–2550

Yamauchi Y, Ogawa M, Kuwahara A, Hanada A, Kamiya Y, Yamaguchi S (2004) Activation of gibberellin biosynthesis and response pathways by low temperature during imbibition of *Arabidopsis thaliana* seeds. **Plant Cell** 16: 367–378

Yokoyama A, Yamashino T, Amano YI, Tajima Y, Imamura A, Sakakibara H, Mizuno T (2007) Type-B ARR transcription factors, ARR10 and ARR12, are implicated in cytokinin-mediated regulation of protoxylem differentiation in roots of *Arabidopsis thaliana*. **Plant Cell Physiol** 48: 84–96

Zhang K, Novak O, Wei Z, Gou M, Zhang X, Yu Y, Yang H, Cai Y, Strnad M, Liu CJ (2014) *Arabidopsis* ABCG14 protein controls the acropetal translocation of root-synthesized cytokinins. **Nat Commun** 5: 3274

Zhao C, Craig JC, Petzold HE, Dickerman AW, Beers EP (2005) The xylem and phloem transcriptomes from secondary tissues of the *Arabidopsis* root-hypocotyl. **Plant Physiol** 138: 803–818

SUPPORTING INFORMATION

Additional Supporting Information may be found online in the supporting information tab for this article: http://onlinelibrary.wiley.com/doi/10.1111/jipb.12486/suppinfo

Figure S1. *35S::ICA* shows increased shoot biomass compared with Col-0

(A) The final stem height is longer in *35S::ICA* than in Col-0 plants ($n = 10$). **(B, C)** The weight of inflorescence stem significantly is increased in *35S::ICA* compared with that in Col-0. Fresh **(B)** and dry **(C)** weight were measured at the first ($n \geq 6$) or sixth silique stage ($n \geq 4$). **(D)** *35S::ICA* enhances the growth of vegetative internode and axillary stems, largely accounting for the increased dry weight of the inflorescence stem. Dry weight was measured at the sixth silique stage ($n = 9$). **(E, F)** The weight of mature leaves is significantly increased in *35S::ICA* compared with that in Col-0. Fresh **(E)** and dry **(F)** weight were measured at the first ($n \geq 6$) or sixth silique stage ($n \geq 4$). **(G, H)** Total weight of shoot is also increased significantly in *35S::ICA* compared with that in Col-0. Fresh **(G)** and dry **(H)** weight were measured at the first ($n \geq 6$) or sixth silique stage ($n \geq 4$). In all data, asterisks denote statistically significant differences from Col-0 using a Student's *t*-test ($^{**}P < 0.01$, $^{***}P < 0.001$). Error bars indicate SE. All experiments were performed at least three times using biologically independent samples.

Figure S2. *35S::ICA* does not show distinct growth phenotypes in the root

(A, B) No difference in the length **(A)** and cell number **(B)** of meristemic zone in the root apical meristem (RAM) is shown in *35S::ICA* compared to Col-0. RAM size was measured as the distance and cell number between the quiescent center (QC) and the first extending cortex cells in 6-day-old seedlings. **(C, D)** The main root length **(C)** and diameter **(D)** are not affected in *35S::ICA*. These traits were measured using the light microscope in 6-day-old seedlings. Error bars indicate SE ($n = 5$).

Figure S3. Endogenous cytokinin (CK) levels are altered in *35S::ICA*

CK levels were measured at various tissues at the sixth silique stage. iP-type CK is N^6-(Δ^2-isopentenyl) adenine and its conjugates, cZ-type CK is *cis*-zeatin and its conjugates, and tZ-type CK is *trans*-zeatin and its conjugates. U1, the uppermost 1 cm of vegetative internode; VI, the other vegetative internodes except U1; II, inflorescence internode; AS, axillary stem; CL, cauline leaves; RL, rosette leaves. Asterisks denote statistically significant differences from Col-0 using a Student's t-test ($^{*}P < 0.05$, $^{**}P < 0.01$, $^{***}P < 0.001$). Error bars indicate SE ($n \geq 3$).

Figure S4. Cytokinin-inducible genes are mostly upregulated in *35S::ICA* based on microarray analysis

Values (fold change) correspond to $\log_2$ ratio of expression from *35S::ICA* (M) and Col-0 (C) *Arabidopsis* plants.

Figure S5. *ica*, an *ICA* knockdown mutant, shows decreased growth phenotypes in the inflorescence stem

(A) Schematic illustration of T-DNA insertion in the *ica* mutant. The black and white boxes indicate exon and UTR regions. The black line in 5′ UTR region indicates intron. **(B)** Transcripts of *ICA* are significantly decreased in the *ica* mutant. Total RNA was isolated from inflorescence stems at the first silique stage. *UBQ1* was used for normalization. **(C–F)** Stem diameter **(C)** and height **(F)** of *ica* are similar to those of Col-0 at the first silique stage, but the total length **(D)** and number **(E)** of vegetative internodes are significantly reduced in *ica* compared to Col-0. **(D)** The total length was measured from the ground to the first uppermost vegetative node. **(B–F)** Asterisks denote statistically significant differences from Col-0 analyzed using a Student's *t* test ($^{*}P < 0.05$, $^{***}P < 0.001$). Error bars indicate SE ($n \geq 7$). All experiments were performed at least three times using biologically independent samples.

Table S1. Endogenous levels of cytokinins in Col-0 and 35S::ICA during shoot development

Phytohormone levels were measured in various tissues at different vegetative stages and the sixth silique stage. Values are represented as average $\pm SE$ ($n \geq 3$), except where labeled. Asterisks denote statistically significant differences from Col-0 using a Student's *t*-test ($^{*}P < 0.05$, $^{**}P < 0.01$, $^{***}P < 0.001$). [a]data only detected in one tissue from three and nine biological replicates, respectively. gFW, gram fresh weight; dos, day-old seedling; U1, uppermost 1 cm tissue of vegetative internode; VI, other vegetative internodes except U1; II, inflorescence internode; AS, axillary stem; CL, cauline leaves; RL, rosette leaves; tZ, *trans*-zeatin; tZR, tZ riboside; tZRPs, tZ ribotides; cZ, *cis*-zeatin; cZR, cZ riboside; cZRPs, cZ ribotides; DZ, dihydrozeatin; DZR, DZ riboside; DZRPs, DZ ribotide; iP, N^6-(Δ^2-isopentenyl) adenine; iPR, iP riboside; iPRPs, iP ribotides; tZ7G, tZ-7-N-glucoside; tZ9G, tZ-9-N-glucoside; tZOG, tZ-O-glucoside; cZOG, cZ-O-glucoside; tZROG, tZR-O-glucoside; cZROG, cZR-O-glucoside; DZ9G, DZ-9-N-glucoside; iP7G, iP-7-N-glucoside; iP9G, iP-9-N-glucoside; N. D., indicates not detected.

Table S2. Endogenous levels of gibberellins (GAs), auxins (IAAs), and jasmonic acid (JA) in Col-0 and *35S::ICA* at the sixth silique stage

Phytohormone levels were measured in various tissues at the sixth silique stage. Values are represented as averages $\pm$ SE ($n = 9$), except where labeled. Asterisks denote statistically significant differences from Col-0 using a Student's *t*-test ($^{*}P < 0.05$, $^{**}P < 0.01$, $^{***}P < 0.001$). [a]data only detected in one tissue from nine biological replicates. U1, uppermost 1 cm tissue of vegetative internode; VI, other vegetative internodes except U1; II, inflorescence internode; AS, axillary stem; CL, cauline leaves; RL, rosette leaves. gFW, gram fresh weight; N. D., not detected. IA-Ile + IA-Leu, IA-Phe, IA-Trp, GA_1, GA_3, and GA_8 were also measured, but not detected.